Macromolecules

ARTICLE

pubs.acs.org/Macromolecules

Self-Assembly of Diblock Copolymer on Substrates Modified by Random Copolymer Brushes

David M. Trombly, Victor Pryamitsyn, and Venkat Ganesan*

Department of Chemical Engineering, University of Texas at Austin, Austin, Texas 78712, United States

ABSTRACT: We model the self-assembly of a diblock copolymer thin film in contact with a random copolymer brush using self-consistent field theory employing a quenched distribution for the brush chains. We focus on the regime of parameters where the diblock copolymers exhibit lamellar morphologies, and study the alignment behavior of the lamellar morphologies on the grafted substrates. Our results reveal a templating of the self-assembly morpology by the brush chains. We find two novel features of this templating behavior: The ends of the grafted chains rearrange themselves to create a more favorable interface, an effect which is present in both the parallel and perpendicular morphologies, and is enhanced with increasing blockiness of the sequences of the random copolymer. In addition, the brush chains may splay laterally in perpendicular morphologies and enrich the interface even further in the favorable component. The latter feature leads to nontrivial free energy differences between the parallel and perpendicularly aligned lamellae on the grafted surface. We explicitly find the parametric window for the stability of perpendicular lamellae and compare against the trends suggested by surface energies of the pure homopolymeric components. Such comparisons indicate that viewing the grafted surface purely in terms of the surface energies of the components of the diblock copolymer may not necessarily capture the stabilities of the parallel and perpendicular morphologies.

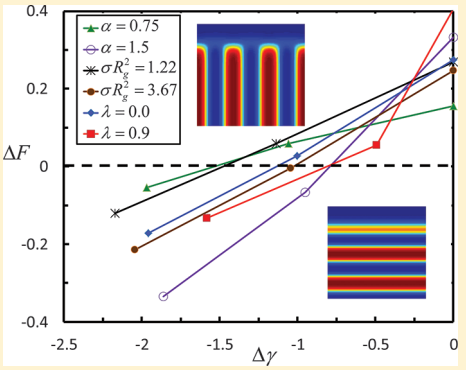

I. INTRODUCTION

The self-assembly behavior of di- and multiblock copolymers has attracted significant attention in both fundamental and technological contexts. Among the many different morphologies exhibited by block copolymers, perpendicularly aligned lamellar and cylindrical phases of diblock (AB) copolymers have constituted an active focus in the design of semiconductor materials. A key challenge in the success of such efforts is to be able to obtain perpendicularly aligned self-assembled structures that are free from defects. The latter in turn requires substrates which are energetically "neutral," i.e., which do not exhibit a preference for either of the components. Indeed, if the substrate exhibits a preference for one of the components, then it is more likely that this component will wet the substrate, resulting in the formation of parallel aligned phases. Unfortunately, however, many of the commonly employed substrates do exhibit an energetic preference for one of the blocks, necessitating additional strategies to render them neutral to the different components.

In relation to the above, experimentalists have pursued a variety of methods to induce the formation of perpendicularly aligned phases, such as the patterning of surfaces[1] and the use of electric fields to align the morphologies.[2,3] One such strategy which has been pursued for achieving perpendicular lamellae is to modify the interactions between the polymers and the substrate by using grafted polymers. Mansky et al. first demonstrated the viability of this approach to control the alignment and self-assembly of diblock copolymers.[4] Explicitly, they used a styrene (S) and methyl methacrylate (MMA) random copolymer (P(S-*r*-MMA)) brush with varying compositions of S and MMA as the substrate for alignment of the block copolymer. By measuring the surface energies of the homopolymers polystyrene (PS) and poly(methyl methacrylate) (PMMA) on the brush as a function of the composition of S and MMA in the brush, these authors showed that the surface energies of the different components with the brush substrate could be tuned by modulating the compositions of the brush copolymer.[4] More pertinently, they identified a regime called the "neutral window," for which the grafted substrate exhibited approximately equal preference for S and MMA blocks, and showed that in such a regime the substrate was effective in creating perpendicular aligned phases.[4,5] However, since the free surface had an affinity for the PS, parallel morphologies still tend to be formed near the free surface.[5] The same authors later used an end-functionalized random copolymer segregated to the polymer−air interface to induce perpendicular lamellar structures throughout the film.[6] Subsequent work has advanced this idea to other systems by using alternative strategies such as cross-linking agents and/or grafting chemistries.[7,8]

Complementing the above experimental efforts, there has also been extensive modeling and simulation work focusing on the self-assembly behavior of di- and multiblock copolymer films. While early work of Turner, Mayes, and others used simple scaling-type theories,[9−11] later research by Shull, Matsen, Balazs,

Received: September 12, 2011
Revised: November 7, 2011
Published: November 30, 2011

and co-workers pioneered a more direct numerical approach based on polymer self-consistent field theory (SCFT) which helped to shed light on the different parameters underlying the self-assembly behavior of block copolymers.[12−14] These researchers modeled diblock copolymer thin films bounded by homogeneous substrates with energetic preference for one of the blocks. Using such a model, it was confirmed that substrates displaying an energetic preference for one of the components tended to induce the formation of parallel aligned lamellar phases. In contrast, for a neutral substrate, a perpendicular arrangement was always preferred or degenerate with parallel arrangements. Such studies also demonstrated the critical role played by the film thickness in modulating these trends for confined polymer films. Explicitly, in parallel aligned phases confined to thicknesses which are incommensurate with the equilibrium lamellar thickness, they showed that there is a competition between the energetic gain arising from the interactions with the substrate and the entropic costs that may be incurred in deforming the lamellae to fit them within the confined space. This competition results in the formation of perpendicularly aligned phases for certain ranges of thickness even for preferential substrates. Similar behavior was also shown using Monte Carlo simulations.[15,16] Subsequent work has extended the above developments by focusing on the cases of asymmetric diblock copolymers,[17] multiblock copolymers,[18−23] the impact of patterned hard surfaces[24−28] and the effects of surface roughness.[28,29] More recent studies of diblock copolymer thin films bounded by homogeneous surfaces has elucidated the plethora of mixed morphologies that may occur as a function of the complex system parameter space.[30]

At the other end of the spectrum, much modeling work has also been accomplished in the context of the interfacial properties of grafted polymers. This has included studies of grafted diblock copolymers,[31−37] Y-shaped copolymers,[38] and systems with blends of homopolymers.[39−42] Grafted statistical copolymer systems such as grafted gradient copolymer melts[43] and random copolymers in a selective solvent[44] have also been studied. In order to further modeling effects on grafted statistical copolymers and by analogy to the early work of Mansky et al., we recently completed a study of a random copolymer brush in contact with a homopolymer melt and studied the interfacial energies as a function of different parameters.[45] Our results showed that an important phenomena that manifests in such situations is the possibility for the brush chains to rearrange their ends to expose a more "enriched" fraction of the favorable phase to the melt in contact. In our earlier work, we showed that the surface energies between the hompolymer melt and the brush is crucially dependent upon this rearrangement effect.[45]

Both the experimental work of Mansky et al.[4] as well as our previous work on the interfacial properties of random copolymer brushes have used the surface energies of A and B homopolymers on random copolymer brushes to draw conclusions about the expected behavior for diblock copolymer alignment on such substrates. While this is a reasonable strategy, such an approach however leaves unaddressed many interesting issues relating to the synergistic aspects between the self-assembly of the block copolymer and the grafted copolymers. Explicitly, grafted copolymers differ from the hard walls modeled previously in that they represent a soft substrate which can potentially modulate their thicknesses to accommodate the self-assembly of the block copolymers. A more interesting possibility in the case of random copolymer brushes is that they can create chemical inhomogeneities in both the lateral and normal direction (relative to the substrate), and thereby modulate the surface energies to either template or accommodate the self-assembled structures of the block copolymer film. These considerations prompt the question of whether there indeed is a "strict" correspondence between the surface energies and the actual alignment of the diblock copolymer, and whether this alignment matches the behavior predicted for self-assembly of diblock copolymers on smooth, hard walls.

Only very few articles have modeled the self-assembly characteristics of block copolymers on grafted surfaces. Ren and co-workers considered the self-assembly of asymmetric block copolymer melts on homopolymer brushes using polymer self-consistent field theory (SCFT).[46] They found that, upon changing the grafting density, the system alternated between lamellar and spherical morphologies and that templating of the grafted homopolymer occurred in response to the spherical phases. However, these studies did not address the issues regarding the connection between surface energies and the self-assembly morphologies. Moreover, the possibility of self-assembly driven chemical inhomogeneities in the grafted layers is a feature unique to the context of random copolymer and multicomponent polymer brushes which does not have an analogue in the homopolymer context. To address these issues, in a recent short communication we presented results which went beyond our previous work on the interfacial properties of random copolymers by modeling directly the self-assembly of block copolymers on grafted copolymer brushes.[47] Our framework used a detailed numerical implementation of polymer SCFT and for a 2-D system while invoking a *quenched sequence configuration* of random chains. Our results indicated novel synergy between the block copolymer self-assembly and the inhomogeneities induced in the brush. This feature rendered the self-assembly in our system to be much more complex than the behavior observed for block copolymers confined by smooth, hard walls. The latter was also reflected in the quantitative comparisons we presented between the surface energies and the stabilities of perpendicularly and parallel aligned phases.

In this article, we elaborate the details of the model used in our shorter communication[47] and also present results quantitatively exploring the influence of various parameters, which include grafting densities, film thicknesses, composition of the random copolymer and the blockiness of its chemical sequences. To minimize the overall number of parameters to be studied, we hold constant the interaction between dissimilar segments (quantified by the Flory parameter χ) and focus only on the case of a "symmetric" diblock copolymer, which forms lamellar phases. Moreover, we also assume that the confinement of the film is "symmetric" and has identical grafted layers on both surfaces. In order to isolate the specific effect of the random copolymers, we assume that the substrate on which the polymers are grafted is a "neutral" surface for the two components of the diblock copolymer. Using the above model and assumptions, we study the self-assembly of the block copolymers upon random copolymer brushes.

The rest of the article is arranged as follows: In section II, we explain key details of our theoretical and numerical methods. In section III, we discuss some key relevant morphological features arising in the parallel and perpendicular self-assembly of block copolymers on the grafted layers. In section IV we present results pertaining to the "neutral window," that is, the parametric regime which leads to perpendicular alignment of the block copolymer. We present an explicit comparison of this regime to the surface energies of the homopolymers on random copolymer brushes and comment on the correspondences and discrepancies. In the Appendix, we elaborate the details of the modeling framework used in this article.

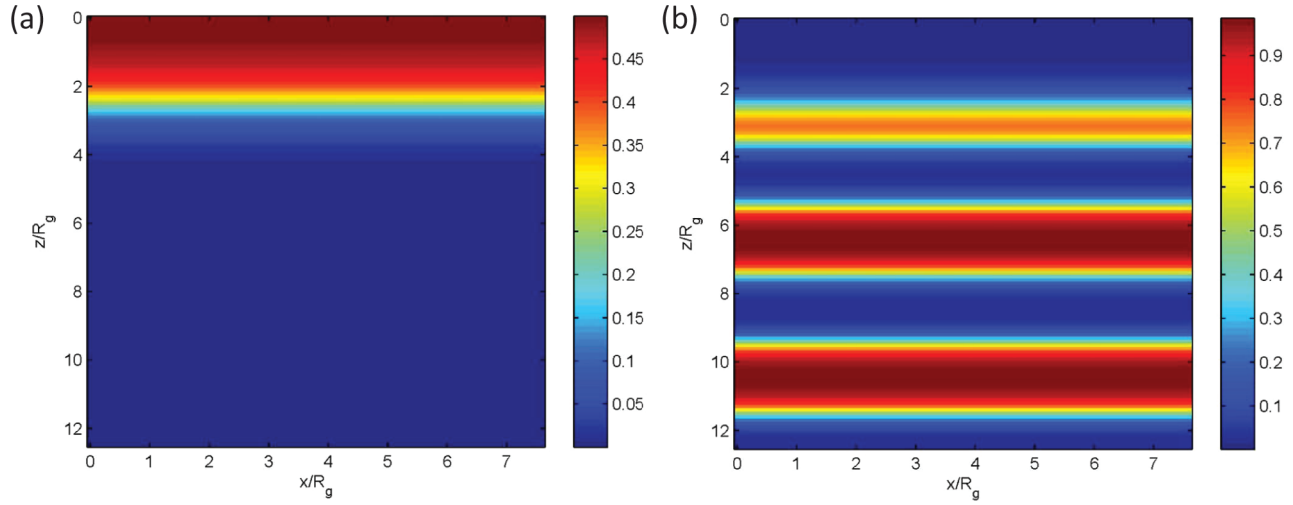

Figure 1. Pictures of parallel lamellar morphology for parameters $\lambda = 0.0$, $\sigma R_g^2 = 2.45$, $\alpha = 1.0$ and $f_{brush} = 0.5$. (a) Intensity plot of volume fraction of species A of the grafted polymer; (b) Intensity plot of volume fraction of species A of the diblock copolymer.

II. THEORY AND NUMERICAL METHODS

To model the self-assembly of block copolymers on grafted random copolymer surfaces, we use a numerical implementation of polymer self-consistent field theory (SCFT). The details of the formalism for the system under consideration is very similar to that used in our previous work which modeled the behavior of (A) hompolymer films on random copolymer (AB) brushes. To model the behavior of diblock copolymer films, the modifications arise only in the manner in which the densities and volume fraction profiles of different components are computed. Specifically, the presence of the B component in the film adds to the total volume fraction of the B component. To maintain brevity of the text, we relegate the details of the formalism to the Appendix.

In the previous work, since we were only interested in the density profiles and free energies of homopolymers, we could restrict our consideration to one-dimensional variations in the density profiles of the different components. However, in the present context, since we are explicitly concerned with the formation of parallel and perpendicular lamellae, we now solve the resulting self-consistent field theory equations while allowing for inhomogeneities in two spatial dimensions: one normal to the substrate, denoted z, and one tangential to the substrate, denoted x. We solved the diffusion equation resulting in the SCFT in two dimensions using an alternating-direction implicit method. To calculate the surface energies (to compare with the neutral window regimes), we revert back to an one-dimensional formalism where the diffusion equation is solved using a Crank−Nicholson method in only the z dimension. For our two-dimensional calculations, the spatial dimensions are resolved on a mesh size of $\Delta x = \Delta z = 0.1$ and the contour length coordinate s is resolved on a mesh size of $\Delta s = 0.005$. Admittedly, such a mesh is coarse-relative to the parameters commonly used in SCFT studies.[30] However, our choice was necessitated by the numerical complexity accompanying the quenched ensemble of random copolymer chains. For our one-dimensional calculations, the need for free energy results very close to the surface dictates that we solve the equations on a smaller mesh size of $\Delta z = 0.04$ and $\Delta s = 0.0004$. The self-consistent field equations are solved until the maximum change in the self-consistent fields (cf. Appendix for details and notation) was 10^{-2} for w_+ and 5×10^{-3} for w_- . The random copolymer chains grafted to the surface were generated by using a method identical to that employed in our previous work. In the present study, we use a quenched sequence ensemble of 500 chains in our self-consistent field theory. As in the last study, we create chains that have 100 segments, which when $\Delta s = 0.005$ dictates that each segment has two contour mesh (s) points.

From this point in the paper, we choose to denote the average volume fraction of species A in the brush chain by f, the grafting density by σ, the blockiness parameter as λ (see Appendix for details), and the ratio between the chain lengths of the free and grafted chains as α.

III. MORPHOLOGICAL FEATURES OF SELF-ASSEMBLY

We begin the discussion of our results by presenting key features of the parallel and perpendicular morphologies that we observe from our SCFT calculations. In particular, we focus on two key aspects by which the grafted copolymer layers differ from hard surfaces, viz., (i) The ability of the surface to tune the *distribution of the different species* to accommodate the self-assembly of the diblock copolymer. This feature arises from the multicomponent nature of the copolymer and we term this as "chemical templating"; and (ii) The ability of the grafted surface to tune its heights or allow for interpenetration to respond to the self-assembly. This feature arises due to the inherent "softness" of the grafted surface and we term this as "physical templating."

A. Templating of Parallel Lamella. In parts a and b of Figure 1, we display representative volume fraction profiles of the species A within the random copolymer brush and the diblock copolymer for the case when the diblock copolymer exhibits a lamellar phase with parallel alignment. While the displayed profiles correspond to the situation where the A component is in contact with the brush, since the random copolymer brush shown in Figure 1 corresponds to a case of $f = 0.5$, we expect the case with B component in contact with the brush to be equally possible. We observe from parts a and c of Figure 1 that there are no perceptible *lateral* inhomogeneities in the brush profiles, whence we use the in-plane averaged volume fraction profiles to quantify the details of the morphology.

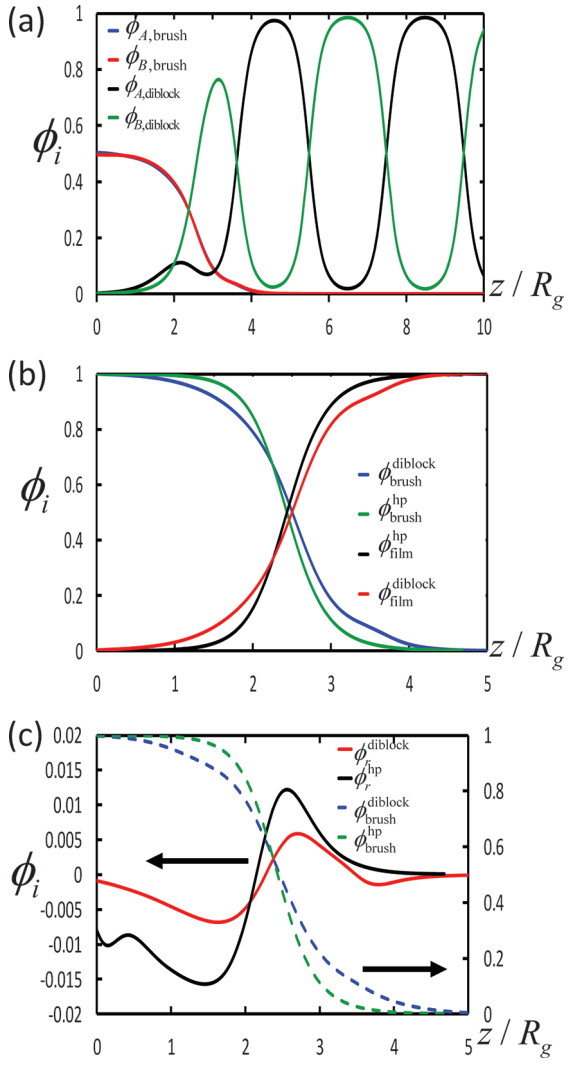

Figure 2. In parts a−c parameters correspond to $\lambda = 0.0$, $\sigma R_g^2 = 2.45$, $\alpha = 1.0$ and $f_{brush} = 0.5$. (a) Composition profiles of different components of a diblock copolymer in parallel alignment on the grafted surface (z denotes the coordinate normal to the surface). (b) A comparison of the overall density profiles of brush and film components for homopolymer and diblock copolymer films. (c) A comparison of ϕ_r for homopolymer and diblock copolymer films. The brush volume fraction profile (secondary Y axis) is illustrated in dashed lines to highlight the interfacial zone.

In Figure 2a, we display the in-plane averaged composition profiles for parallel aligned diblock copolymers on symmetric random copolymer brushes ($f = 0.5$). We observe two features which exemplify the main features of self-assembly upon grafted multicomponent polymers: (i) The presence of significant interpenetration between the brush and the overlaying film, which highlights the "soft" nature of the grafted surface. The latter is clearly seen in the broad interfacial zone between the brush and the film components displayed in Figure 2b. (ii) There is a segregation between the A and B components of the brush, which leads to an enrichment of the A component (of the brush copolymer) in the interfacial zone between the brush and the overlaying film. The latter is most clearly evident in the enrichment function $\phi_r = \phi_{A,brush} - \phi_{B,brush}$ displayed in Figure 2c, which is seen to become positive in the interfacial region. To compensate for this

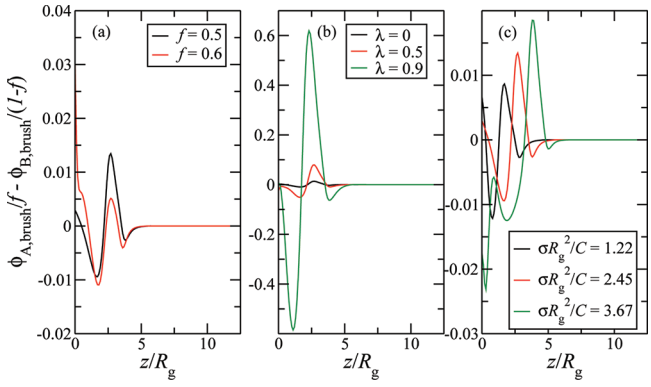

Figure 3. Compositional enrichments for different parametric conditions of the grafted copolymer surface: (a) varying f; (b) varying λ; (c) varying $\sigma R_g^2/C$. Unless otherwise stated, $\sigma R_g^2/C = 2.45$, $f_{brush} = 0.5$, and $\lambda = 0$. Diblock composition $f_{diblock} = 0.5$. Chain lengths and segment interactions are defined by $\alpha = 1$ and $\chi N = 20$.

enrichment, ϕ_r is seen to become negative in the interior regions of the brush, indicative of the depletion of A component in such regions. This enrichment is a manifestation of a "chemical" templating effect, was also seen in our previous work[45] which examined the behavior of homopolymer melts in contact with random copolymer brushes. In that case, we showed that, even for a symmetric brush ($f = 0.5$), the chain ends of the random copolymer can rearrange themselves to present an enriched amount of the enthalpically similar component in the interfacial region where the brush overlaps with the free polymer. Such a rearrangement was argued to reduce the enthalpic component of the interfacial energies while costing little to nothing in the entropic component.

What is the role of self-assembly of the block copolymer upon the above-discussed features ? To address this issue, in Figure 2, parts b and c, we compare the above morphological features with the corresponding results for a homopolymer film on an identical brush. While there are similarities seen between the behaviors of homopolymer and diblock copolymer films, quantitative differences are also evident. Explicitly, we observe that the diblock copolymers exhibit larger interpenetration with the brush (evident in the larger overlap between the brush and film volume fraction profiles). Moreover, from Figure 2c, we observe that diblock copolymers exhibit different magnitudes of "enrichment" of the brush component (the peak for the diblock film occurs at $\phi_r = 0.0059$, whereas it occurs at $\phi_r = 0.0122$ for the homopolymer case). In our earlier communication,[47] we demonstrated that such morphological differences lead to significant differences when comparing the surface energies of the parallel aligned lamella with that of the homopolymer films. Since the focus of the present article is on the comparisons between parallel and perpendicular aligned morphologies of the diblock copolymer, we refrain from elaborating on the comparisons to the homopolymer case further.

Influence of the Characteristics of the Grafted Layer. In Figure 3, we present results which quantify the manner in which the above-discussed "chemical templating" rearrangement effect varies with different parameters of the grafted layer. Figure 3a displays the variation of the rearrangement effect with increasing f, under which conditions the brush and the overlaying component of the diblock copolymer become more chemically similar. In our earlier article, we showed that the chemical rearrangement effect can in general (for $f \neq 0.5$) be quantified through the quantity $\phi_{A,brush}(z)/f - \phi_{B,brush}(z)/(1-f)$, which corresponds to the

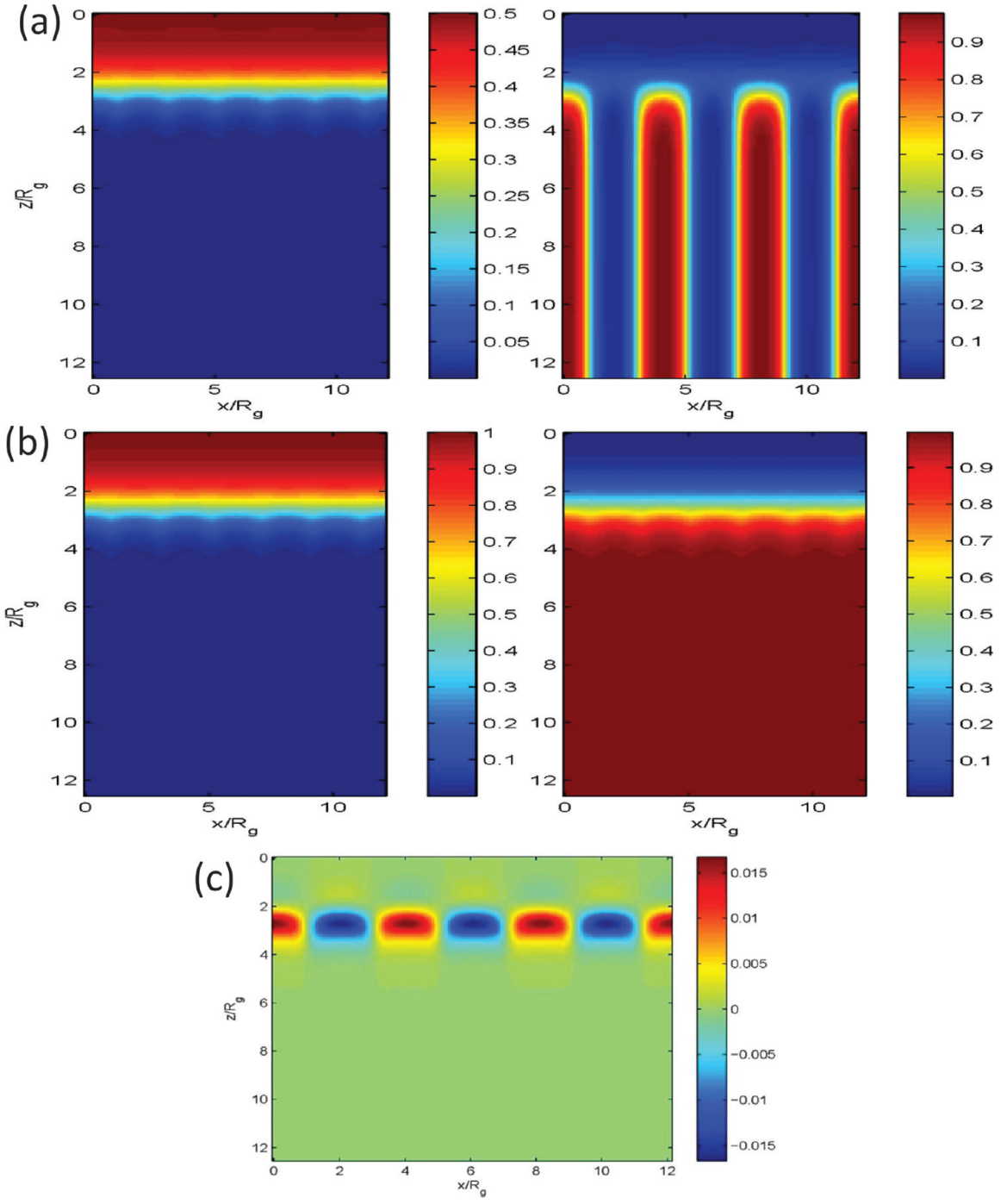

Figure 4. (a) Intensity plot of the volume fraction of the A component in the brush (left) and the diblock copolymers (right). (b) Intensity plot of the total volume fraction of the brush (left) and the diblock copolymers (right). (c) Intensity plot of the compositional enrichment effect. The results correspond to parametric conditions: $f_{brush} = 0.5$. $\sigma R_g^2/C = 2.45$, and $\lambda = 0$. Diblock composition $f_{diblock} = 0.5$ Chain lengths and segment interactions are defined by $\alpha = 1$ and $\chi N = 20$. Film thickness is $12.5R_g$, which is the location of the minimum in energy of parallel morphology for three lamellaes.

amount of enrichment in species A that occurs in the brush relative to the average volume fraction of each species. As was observed in our previous work with random copolymer brushes and homopolymer melts, the enrichment of species A (i.e., the chemical templating effect) becomes less pronounced as f increases, evidenced by the decreasing magnitude of the positive peaks toward the right of the plots. This trend is easily understood by noting that with increasing f, the brush copolymer itself becomes more similar to the polymer in contact with it. Hence, there is a corresponding decrease in the amount of enrichment achievable in the interfacial region by rearranging the chains ends. Moreover, in such conditions the grafted copolymer is chemically more similar to the overlaying homopolymer, and hence there is inherently a favorable enthalpic interaction between them. While chain rearrangements may contribute further to these favorable interactions, they are expected to do so only at a secondary level and therefore there is a reduced propensity for such behavior.

dx.doi.org/10.1021/ma202075d |*Macromolecules* 2011, 44, 9867–9881

In Figure 3b, we display the effect of increased blockiness (with f fixed at 0.5) on the rearrangement within the random copolymer brush. Similar to the results presented in our previous article for the case of a random copolymer brush in contact with a homopolymer, the rearrangement effect is seen to depend sensitively on the blockiness of the random copolymer sequences. Moreover, it is seen that for the most blocky sequences ($\lambda = 0.9$), the interfacial enrichment can be substantial relative to the average volume fractions of the species. This behavior, which also parallels results shown in our earlier article, can be explained by noting that since the blockier polymers contain longer blocks of identical component, rearranging their chain ends allow for more substantial enrichment of the preferred component.

Finally, in Figure 3c, we display the affect of changing grafting density upon the chain rearrangement. With increasing grafting density, we observe that the enrichment in A segments also exhibit a monotonic increase (seen in the magnitude of the peaks of $\phi_{A,brush}(z)/f - \phi_{B,brush}(z)/(1-f)$ in the interfacial region). Increasing grafting density enhances the number of chain ends per unit area. We hypothesize that the latter allows for a larger enrichment in the interfacial zone as seen in Figure 3c.

In summary, in this section we discussed "chemical templating" phenomena arising in the brush copolymer due to the presence of an overlaying parallel aligned diblock copolymer. Explicitly, we demonstrated that chemical templating arises through a rearrangement of the chains to enrich the brush in the component of the diblock copolymer, which is at the interface. The parametric dependencies of this chain rearrangement effect were shown to be qualitatively consistent, albeit quantitatively different from the results presented in an earlier article for the interface of a random copolymer brush and a homopolymer melt.

B. Templating of Perpendicular Morphologies. In contrast to the behavior discussed for the case of parallel lamella phases, templating of perpendicular morphologies is expected to be even richer due to the possibility of both normal and lateral inhomogeneities. Moreover, within the context of tangential inhomogeneities, two situations may arise: (i) Inhomogeneities in the heights of the grafted layer (referred to earlier as "physical templating"). (ii) A compositional or chemical templating similar to that observed in the context of the lamella phases aligned in the parallel direction. Below we present evidence for the occurrence of both of these possibilities and discuss their dependence on different parameters of the grafted layer.

Self-Assembly on Symmetric Brush Copolymers. In Figure 4a, we display representative composition profiles of the A components in the diblock copolymer and the random copolymer brush for the case where the diblock copolymer lamellae are aligned perpendicular to the substrate. It can be observed that the lamellae formed by the diblock copolymer are rounded at the edges in the region which are in contact with the brush. This feature is seen to manifest more clearly in the results displayed in Figure 4b, which depicts the total volume fractions of the diblock copolymer and the brush component. The latter quantifies the structure and height of the brush and is seen to display periodical inhomogeneities with peaks in the regions corresponding to the location of the interfaces between the A and B components of the diblock lamellae. Taken together, the preceding observations indicate a "physical templating" of the brush driven by the rearrangement of the grafted layer in an inhomogeneous manner to accumulate more material from the brush at the AB interface of the lamellae of the diblock copolymer.

Before we discuss the origins of the above behavior, we note another aspect of self-assembly in perpendicular alignment. Specifically, in the plot of the segmental enrichments (defined as $\phi_A/f - \phi_B/(1-f)$ of the brush component) displayed in Figure 4c, it is seen that the composition profiles of the A and B components in the brush are both enriched in the regions where they are in contact with the respective phases. A more nontrivial aspect of this chemical templating behavior is in a comparison of the magnitudes of the enrichments observed in the interfacial region for perpendicularly and parallel aligned lamellae. Explicitly, it is seen that for the perpendicular alignment the magnitude of A (and B) enrichment in the interfacial region is ~0.017, which is larger in magnitude than the enrichment 0.013 noted in the corresponding result for parallel lamellae.

We hypothesize that the origins of the above observations can be traced back to the statistics of the sequences in the grafted chains and the manner in which they rearrange their ends to reduce the enthalpic cost of the interface between the diblock copolymer lamella and the grafted layer. The presence of chemical templating of the diblock copolymer is easiest to understand as a generalization of the behavior seen for the parallel lamellae. Explicitly, the chain ends now rearrange so as to present an enriched phase of the appropriate component at the interface. Since the components of the diblock copolymer are arranged in a periodic manner, the rearrangement and the enrichment of the chain ends also exhibit a periodic profile.

We note that by a mechanism similar to the above considerations, by rearranging its chain ends, the grafted layer can present "neutral" portions of the chains (i.e., which exhibit equal affinity to both A and B components) to the diblock copolymer. The latter can potentially reduce the energy costs at the interfaces of a diblock copolymer by acting like a surfactant. We believe that such a mechanism is responsible for the "physical templating" seen at the interfacial locations of the diblock lamellae see in Figure 4, parts a and b. This is also confirmed by the gaps seen in the enrichment plots displayed in Figure 4c, which are indicative of a lack of enrichment and a more uniform distribution of A and B monomers of the brush at the lamellar interfacial locations of the diblock.

What are the origins of the enhanced rearrangement (relative to parallel alignment) in chemical templating for the perpendicular lamellae? We believe that this arises from a conformational rearrangement of the chains. Explicitly, the grafted chains which are in contact with the A portion of the block copolymer, but whose ends are enriched in the B component have two options: (i) They can move to the interior of the layer, as they do in the case of parallel arrangement. (ii) If they are sufficiently close to the B portion of the lamellae, then they can splay and contribute to the enrichment of B component in the B portion of the diblock copolymer. We believe that the mechanism ii leads to an "enhanced" enrichment in the case of perpendicular lamellae. A quantitative verification of this splaying hypothesis requires an explicit calculation of the two point propagator, which is numerically cumbersome. Instead, below we present the morphological characteristics for other parametric conditions and argue that they support our proposal.

The first evidence for the above-proposed mechanistic explanations is furnished by considering the self-assembly upon a more blocky random copolymer brush (while keeping f fixed at 0.5), depicted in Figure 5, parts a−c. We observe that the qualitative features of the morphologies in this case are very similar to that of $\lambda = 0$ shown in Figure 4. However, we note three features which distinguish systems with higher blockiness: (i) The magnitude

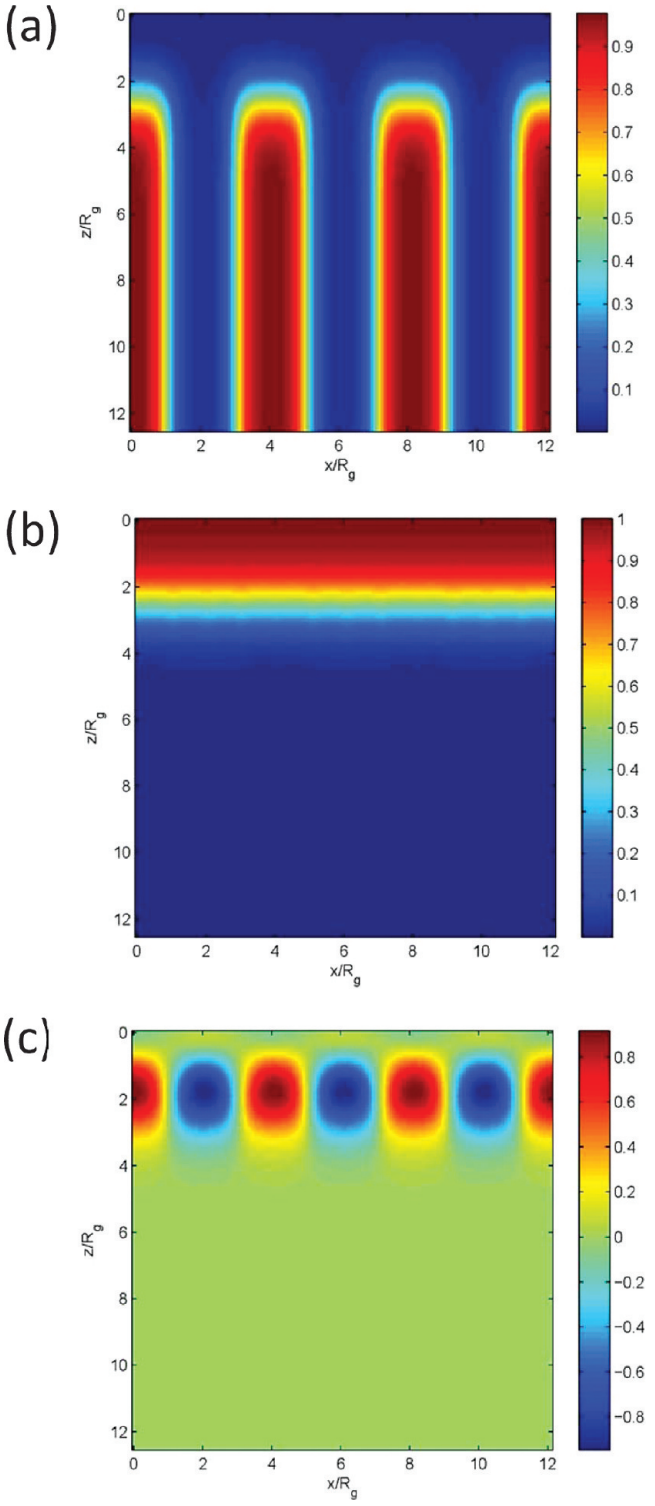

Figure 5. (a) Intensity plot of A component of the diblock copolymer. (b) Intensity plot of the total volume fraction of the brush component. (c) Intensity plot of compositional enrichment effect. Parameters correspond to $\lambda = 0.9$. $\sigma R_g^2/C = 2.45$ and $f_{brush} = 0.5$. Diblock composition $f_{diblock} = 0.5$. Chain lengths and segment interactions are defined by $\alpha = 1$ and $\chi N = 20$. Film thickness is $12.5R_g$, which is the location of the minimum in energy of parallel morphology for three lamellaes.

of the physical templating effect seems diminished and the brush height becomes more uniform in the lateral direction

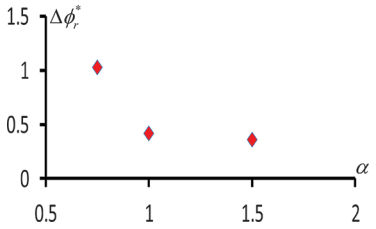

Figure 6. α dependence of the compositional enrichment in the perpendicular aligned morphology relative to the parallel alignment. The quantity $\Delta\phi^*_r \equiv (\phi_r^{perpendicular} - \phi_r^{parallel})/\phi_r^{parallel}$, where $\phi_r^{perpendicular}$ and $\phi_r^{parallel}$ are defined as the peak values in the composition enrichment ϕ_r observed for perpendicular and parallel morphologies, respectively.

(compare Figures 4b and 5b). (ii) The magnitude of the chemical templating becomes more pronounced for the blockier copolymers (compare Figures 4c and 5c. (iii) The differences in the enrichment effect between the perpendicular and parallel phases become more pronounced. Explicitly, the magnitudes of the maximum enrichment are 0.916 and 0.619 for the perpendicular (Figure 5c) and parallel phases (Figure 3c) respectively.

The above observations are consistent with the mechanisms proposed in explaining Figure 4. First, we point out that increasing blockiness leads to chains which have longer sequences of A or B monomers (with, however, the average over the different chains being maintained at $f = 0.5$), and hence less numbers of "neutral" sequences. Consequently, they are expected to be less efficient than the nonblocky chains ($\lambda = 0$, depicted in Figure 4) in modulating the interfacial cost of AB interfaces in diblock lamella, which explains point i above. However, for the same preceding reason, blockier chains allows for an easier and more substantial chain rearrangement and enrichment at the interface, thereby explaining point ii above. Finally, for the same reason, conformational rearrangements of the chains (splaying) is expected to have a more significant effect at enhancing the interfacial enrichment, and is consistent with our observation in point iii above.

A more direct evidence in support of the role of splaying of chains relates to the dependence of the self-assembly characteristics upon the ratio between the chain lengths of the free and grafted chains, α. Explicitly, if the enhanced rearrangement observed in the perpendicular alignment did arise due to the splaying of the chains, we would expect that increasing α would increase the period of the block copolymer phase relative to the brush height and reduce the influence of such conformational rearrangements. In other words, increasing α is expected to render the enrichments in the perpendicular alignment to become more similar to the case of parallel alignment. In Figure 6, we provide evidence from our results that the trends observed in our numerical results do match with this expectation, thereby adding further support to the mechanisms proposed to explain the differences between parallel and perpendicular aligned lamellae.

In summary, the results presented above indicate that the morphological features accompanying the self-assembly in perpendicular alignment shares many characteristics in common with the situation corresponding to parallel alignment. However, a nontrivial aspect of our results is the enhanced enhancement observed in the context of perpendicular alignment. One ramification of this enhanced enrichment is that even when considered at the same conditions of the grafted copolymers, parallel and perpendicular lamellae exhibit different characteristics in the interfacial layer between the block copolymer component and

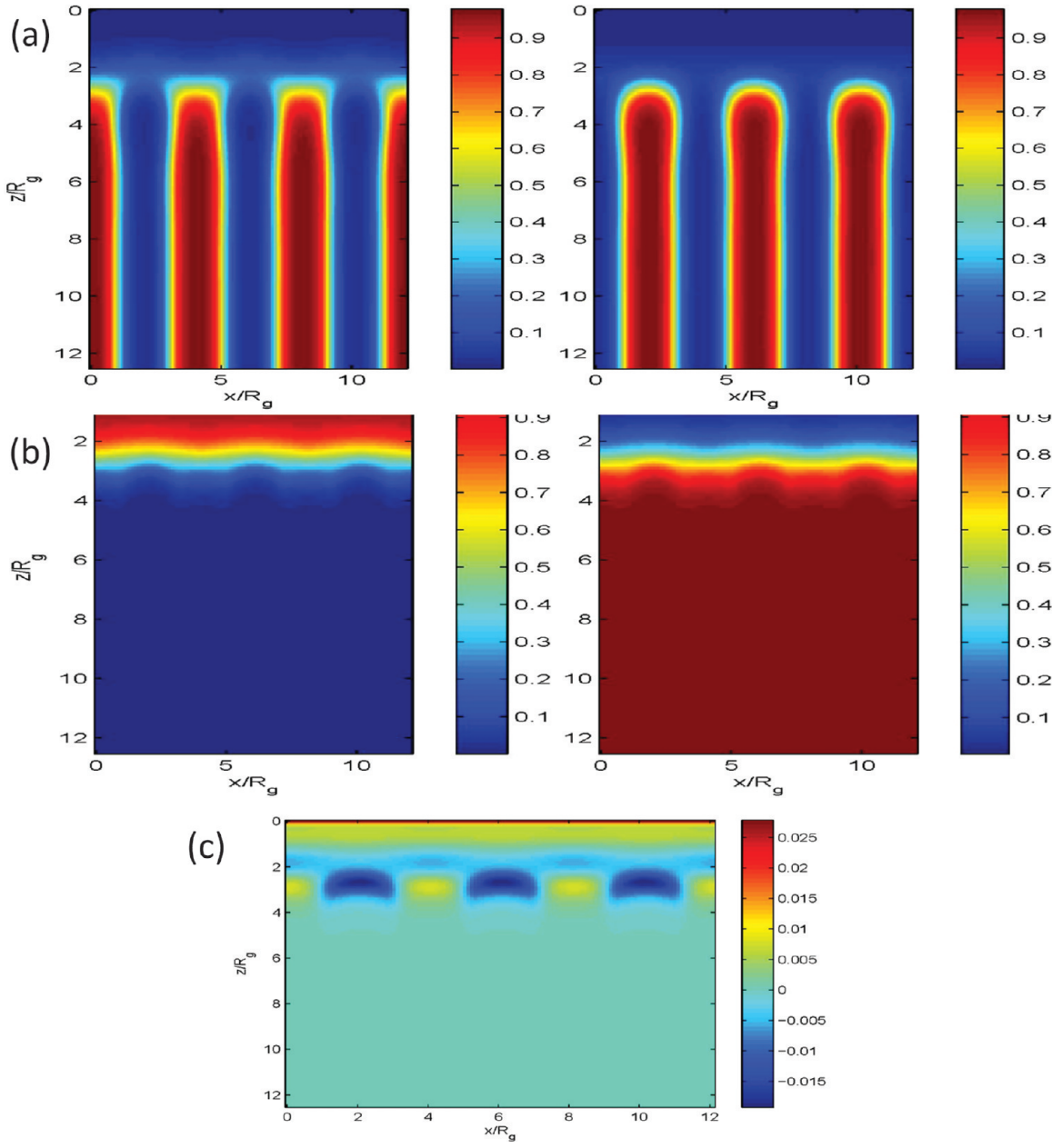

Figure 7. (a) Intensity plot of species A (left) and B (right) components of the diblock copolymer. (b) Intensity plot of the total volume fractions of the brush (left) and diblock copolymer (right). (c) Intensity plot of the compositional enrichment for a perpendicular lamellar morphology at $f_{brush} = 0.6$. $\sigma R_g^2/C = 2.45$, and $\lambda = 0$. Overall, diblock composition $f_{diblock} = 0.5$ Chain lengths and segment interactions are defined by $\alpha = 1$ and $\chi N = 20$. Film thickness is $12.5R_g$, which is the location of the minimum in energy of parallel morphology for three lamellaes.

the grafted polymer. Indeed, the perpendicular lamellae, being the beneficiary of enhanced interfacial enrichment, will have more favorable interfacial interactions with the grafted surface when considered relative to the parallel alignment. In the next section, we show this finding has important consequences for the stability of the perpendicularly aligned phases.

2. Self-Assembly on Nonsymmetric Brush Copolymers. How do the above trends change for a surface comprised of nonsymmetric ($f \neq 0.5$) grafted chains? In Figure 7, we present results displaying the effect of f for a nonblocky ($\lambda = 0$) random copolymer. In comparing these results with the results depicted in Figure 4, we observe the following features: (i) The diblock copolymer lamellae become asymmetric with the A segments of the diblock spreading more on the grafted layer, whereas the B segments reduce their contact with the brush. (ii) The height inhomogeneities in the brush become more pronounced, with the brush exhibiting *relatively* enhanced and lowered heights in regions in contact respectively with the A and B segments of the diblock copolymer. (iii) The rearrangement/chemical templating effects are seen to become more mitigated for the A component whereas it is enhanced for the B component. This is seen by comparing the magnitude of the positive values (representing the enrichment of A) which is 0.017 in Figure 4c, whereas it is 0.008 in Figure 7c. On the other hand, the magnitude of the negative values (enrichment of B) in Figures 4c and 7c are 0.017 and 0.019, respectively.

Much of the above observations can be understood by noting that for $f > 0.5$ the grafted polymer has a higher fraction of A segments (if $f < 0.5$ there is a higher fraction of B segments). Consequently, the grafted surface is by itself preferable to the A segments of the block copolymers and not preferable to the B segments of the block copolymers. In view of this feature, it is not surprising that the lamellae of the diblock copolymers become asymmetric with an enhanced spreading of the A polymers (point i above). However, unlike a hard surface with an inherent surface energy, grafted polymers can modulate the contact between the surface and the B component by an appropriate conformational rearrangements and redistribution of the segments. We believe that the preceding mechanism underlies observation ii above where the grafted chains compress themselves to bring more of their B segments in contact with the B phase of the diblock copolymer. The changes in the rearrangement plots and trends in point iii can be understood by noting that since the brush is as a whole enriched in A segments, there is expected to be less driving force for chain rearrangement driven interfacial enrichment of A segments. Moreover, the magnitude of the A enrichment possible (relative to the average volume fraction of A) also diminishes with increasing f. In contrast, an opposite effect is at play for the B segments in the brush. Explicitly, the region of the brush which is in contact with the B segments of the diblock copolymer experience an unfavorable interaction and hence try to reduce the corresponding enthalpic costs by undergoing chain rearrangements to enrich the interfacial region in B segments. Moreover, the magnitude of the B enrichment possible (relative to the average volume fraction of B) also increases with increasing f. Together, the preceding effects manifest in observation iii noted above.

In summary, the above morphological characteristics indicate novel physical and chemical templating arising during the perpendicular alignment of block copolymer lamellae. In the next section, we develop these considerations more quantitatively by considering the free energies of parallel and perpendicular alignment and the preferred equilibrium alignment.

IV. EQUILIBRIUM ALIGNMENT AND NEUTRAL WINDOWS

In this section, we use a more quantitative framework to examine the self-assembly characteristics of block copolymers on grafted random copolymer surfaces. To set the context for the manner in which we quantify the results, in Figure 8, we display the free energy per unit area (relative to the bulk value) of the random copolymer brush-diblock copolymer thin film system as a function of film thickness for the parallel and perpendicular morphologies for a specified set of parameters. The curves labeled 2, 2.5, and 3 correspond to the number of parallel lamellae in the thickness D (which represents half the confinement width). Perpendicular morphologies are unaffected by the confinement thickness and hence their free energies are independent of thickness. On the other hand, we observe that the free energies for the parallel morphologies show an oscillatory trend as a function of film thickness. Such a behavior has been noted in many earlier studies of diblock copolymers,[9,11,13,14] and can be understood as arising from a mismatch between the preferred lamellar domain spacing and the confinement thickness. We note that for the conditions depicted in Figure 8 the bulk lamellar spacing is $4.0R_g$, which (within the fairly coarse $\Delta(D/R_g)$ we examined) is identical to the distance between the minima noted for the parallel alignment.[14] The latter demonstrates that in this case the random copolymer brush has no effect on the preferred spacing of the lamellae.

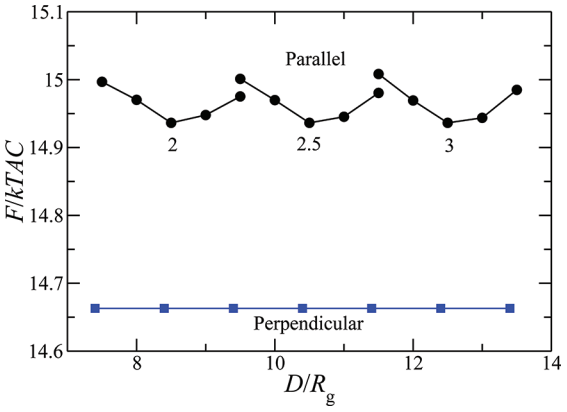

Figure 8. Free energies as a function of film thickness D for a diblock copolymer film in contact with a neutral random copolymer brush-covered substrate. Brush parameters are $\sigma R_g^2/C = 2.45$, $f_{brush} = 0.5$, and $\lambda = 0$. Diblock composition $f_{diblock} = 0.5$. Chain lengths and segment interactions are defined by $\alpha = 1$ and $\chi N = 20$.).

A more nontrivial and an important observation from the plot is that while the depicted conditions correspond to a situation where the grafted surface is "neutral" ($f = 0.5$) to both A and B components, the perpendicular lamella structure seems to be the preferred alignment over the entire range of confinement thickness. In contrast, for block copolymer melts confined by hard, *neutral* surfaces, prior theoretical studies[13] have indicated that the perpendicular morphology is stable, but only due to small free energy differences arising from line tension effects at the interface between the lamellae and the surface. For instance,[15] for stronger segregation conditions corresponding $\chi N = 30.0$, the free energy differences between perpendicular morphology and parallel morphologies were predicted to be $\lesssim 0.1kT$, which is substantially less than the differences seen in Figure 8. The origin of the enhanced stability of perpendicular lamellae in our results can be traced back to the morphological characteristics described in the previous section. Explicitly, we demonstrated that even for a grafting layer with "neutral" characteristics, perpendicular alignment of lamellae was accompanied by an *enhanced* (relative to parallel alignment) chemical enrichment in the brush. This self-assembly driven enrichment is in turn expected to lead to a more favorable interfacial energy between the A and B components of the diblock and their respective contacts with the grafted surface. Additionally, we also showed that there is also the possibility for a "physical templating" of the perpendicular diblock lamellae which reduces the interfacial costs in the diblock copolymer lamellae. We believe that the preceding factors together render the free energies of the perpendicularly aligned lamellae to be lower than the corresponding parallel ones.

With the above understanding, one may enquire what happens when the surface is made more preferential to one of the components. To address this issue, in Figure 9, we display the free energy plots for the above-discussed situation with however the composition of the grafted copolymer surface varied from 0.5 to 0.7 (we zoom in on the confinement thicknesses corresponding to three lamellae). As would be expected upon the rendering the surface to be selective, the free energy of the parallel alignment is seen to be lowered more when compared to the perpendicular alignment.[13,14] It is seen that for $f = 0.6$, the perpendicular lamella

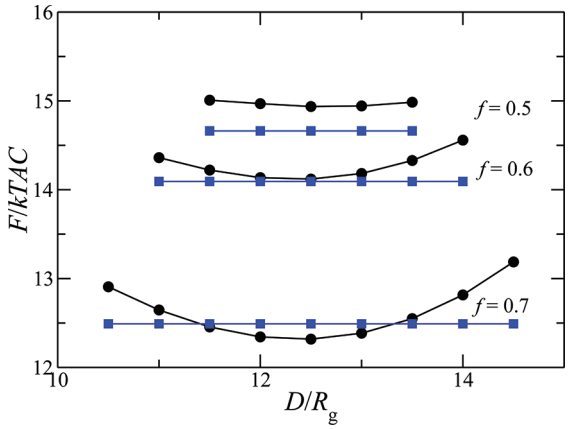

Figure 9. Free energies as a function of film thickness D for a diblock copolymer film in contact with random copolymer brush-covered substrates for average brush compositions $f = 0.5$, 0.6, and 0.7. Brush parameters are $\sigma R_g^2/C = 2.45$, and $\lambda = 0$. Diblock composition $f_{diblock} = 0.5$. Chain lengths and segment interactions are defined by $\alpha = 1$ and $\chi N = 20$.).

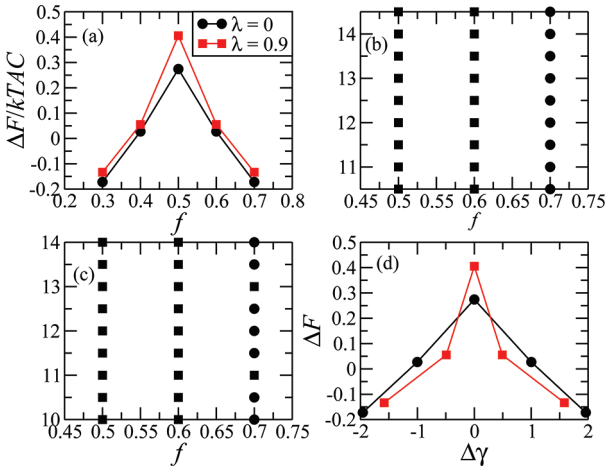

Figure 10. (a) Influence of blockiness (λ) of the random copolymer sequences upon the differences in the free energy between parallel and perpendicular arrangement as a function of f. (b, c) Stable alignment morphologies at different thickness for brushes of different compositions f. Squares denote perpendicular alignment and circles correspond to parallel alignment: (b) $\lambda = 0$ and (c) $\lambda = 0.9$. (d) ΔF as a function of $\Delta\gamma$ for different values of λ. Parameters correspond to grafting density, $\sigma R_g^2/C = 2.45$, diblock composition $f_{diblock} = 0.5$. Chain lengths and segment interactions are defined by $\alpha = 1$ and $\chi N = 20$.

is still the preferred morphology for all thicknesses. However, for $f = 0.7$, it is observed that the parallel alignment now becomes preferred for a range of thickness around its minima. Increasing f further (not shown) is expected to render the parallel lamellae to become the preferred phase for all thicknesses.

Much of the motivation for the present research derives from applications desiring the perpendicular alignment of the lamellar phases. On the basis of the above results, it is evident that there are two questions which relate to the stability of perpendicular phases: (i) For a given set of parameters, what is the critical composition of the random copolymer brush at which the parallel morphology first becomes feasible? Explicitly, this quantifies the critical f_{crit} for the brush copolymer at which the minimum in the free energy curve for parallel alignment becomes lower than that for perpendicular alignment. This quantity is of significant interest for applications since $f < f_{crit}$ delineates the regime for which perpendicular morphologies are preferred independent of the thickness of the grafted layer. We quantify this by considering the quantity $\Delta F = F_{\parallel,min} - F_{\perp}$, where $F_{\parallel,min}$ represents the value corresponding to free energy minima in the parallel alignment. A positive value ΔF corresponds to parametric conditions at which perpendicular alignment is expected to be stable for all confinement thickness. (ii) Another issue related to point i is the following question: For $f > f_{crit}$ what is the range of confinement thickness over which the perpendicular lamellae are still expected to be stable? For instance, in Figure 9, it is seen that even for $f = 0.7$, the perpendicular morphology can be achieved by an appropriate choice of the film thickness. In the following, we also present results for the thickness range of stability of perpendicular lamellae (restricted to $f \leq 0.7$) for different parameters. However, it is to be noted that the latter considerations are expected to hold only for confined films. For free-standing films (such as spun-cast) in such regimes the system would likely opt to form parallel morphologies with islands and holes corresponding to the distinct minima in the free energy curves.

A final issue we consider in the results below pertains to the question raised in the introduction, viz., whether the surface energy differences between the *homopolymeric components* on the grafted surface, can be used to predict the stability of the perpendicular morphologies. Specifically, for a symmetric diblock copolymer, it has been suggested that a key quantity determining the stabilities of parallel and perpendicular alignment of lamellae upon surfaces is[11,14]

$$\Delta\gamma = \gamma_{AS} - \gamma_{BS}$$

where γ_{AS} and γ_{BS} denote the interfacial energies of A and B polymers with the surface (in this case, the random copolymer brush). Of interest is the question whether the stabilities of the perpendicular morphologies are correlated to $\Delta\gamma$. To address the above-raised issue, we probe whether ΔF, representing a measure of the stability of perpendicular lamellae, can be uniquely correlated to $\Delta\gamma$ (in the Appendix, we briefly explain the methodology used to determine $\Delta\gamma$).

A. Effect of Grafted Surface Properties on the Neutral Window. In Figure 10a, we display results for the free energy difference ΔF as a function of f for different blockiness of the random copolymer. We observe that over the entire range of f, the free energy differences between the parallel and the perpendicular phases are larger for more blockier random copolymer brushes. This suggests that the perpendicular phases are expected to exhibit a greater regime of stability when the surface is grafted with blockier copolymers. The latter is also reflected in the thickness dependence of the stabilities of parallel and perpendicular morphologies for $f = 0.5$ and 0.6 depicted in Figure 10, parts b and c, wherein it can be seen that even for $f = 0.7$, the blockier random copolymer ($\lambda = 0.9$) still exhibits thicknesses where perpendicular morphologies are stable. In contrast, for the nonblocky random copolymer ($\lambda = 0.0$), the equilibrium morphologies over the entire range of thickness is seen to correspond to parallel alignment. The preceding results are consistent with the observations we made in comparing Figures 4c and 5c, where it was demonstrated that the differences in the interfacial enrichment between the parallel and perpendicular phases becomes more pronounced with increasing blockiness. Because of such an effect, a more blockier grafted surface is expected to exhibit larger

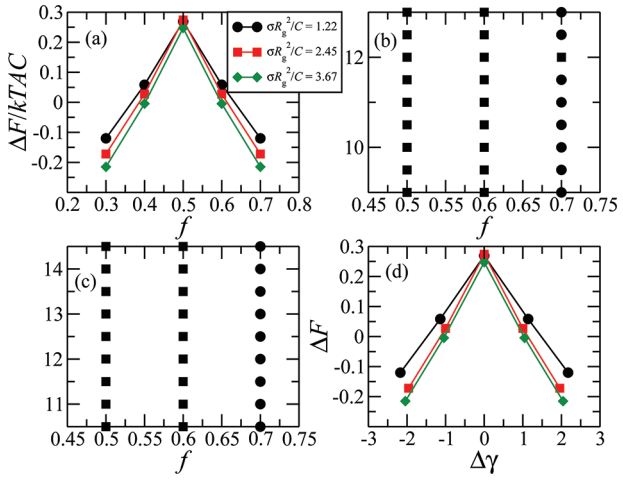

Figure 11. (a) Influence of the grafting density $\sigma R_g^2/C$ of the random copolymer brush upon the differences in the free energy between parallel and perpendicular arrangement as a function of f. (b, c) Stable alignment morphologies at different thickness for brushes of different compositions f. Squares denote perpendicular alignment and circles correspond to parallel alignment: (b) $\sigma R_g^2/C = 1.22$ and (c) $\sigma R_g^2/C = 2.45$. (d) ΔF as a function of $\Delta\gamma$ for different values of $\sigma R_g^2/C$. Parameters correspond to blockiness $\lambda = 0$; diblock composition $f_{diblock} = 0.5$. Chain lengths and segment interactions are defined by $\alpha = 1$ and $\chi N = 20$.

differences between the self-assembly driven surface energies of perpendicular and parallel morphologies—which is consistent with the results of Figure 10, parts a−c.

In Figure 10d, we display the free energy differences ΔF as a function $\Delta\gamma$ for the two different values of blockiness. Interestingly, it is evident that there exists a range of nonzero $\Delta\gamma$ (corresponding to preferential surfaces) wherein perpendicular alignment exists as the preferred morphology. However, it is evident that the correlation between ΔF and $\Delta\gamma$ depends explicitly on the blockiness parameter λ. Moreover, it can be seen that even conditions corresponding to the same differences in the homopolymer surface energies $\Delta\gamma$ can lead to differences in the equilibrium alignment for different brush conditions. The origin of such discrepancies can again be traced back to the previously discussed self-assembly driven modifications of interfacial energies. The magnitudes of the latter are dependent on the physical parameters of the grafted copolymer, and are not captured in the quantity $\Delta\gamma$ which pertains only to the surface energies of the interface between the homopolymer and the brush.

In Figure 11, we display results for the situation when the grafting densities constitute the parameter which is varied (for a nonblocky random polymer, $\lambda = 0$). Unfortunately, due to numerical issues, we had to restrict our exploration in this case to only a limited set of grafting densities. Within the range of grafting densities we probed, it is seen that the lowest grafting density, $\sigma = 1.22$, has a broader neutral window (in the brush composition space), whereas $\sigma R_g^2/C = 2.45$ and $\sigma R_g^2/C = 3.67$ seem to have similar characteristics and a smaller neutral window. The latter trends are also reflected in the thickness dependencies of the neutral window (cf. Figure 11, parts b and c). In Figure 11d, we compare ΔF to the differences in surface energies $\Delta\gamma$. Similar to the effect of blockiness, we observe that there is no unique correlation between ΔF and $\Delta\gamma$. Interestingly, the changes in grafting density seems to have only a small impact upon the free energy differences (between parallel and perpendicular morphologies).

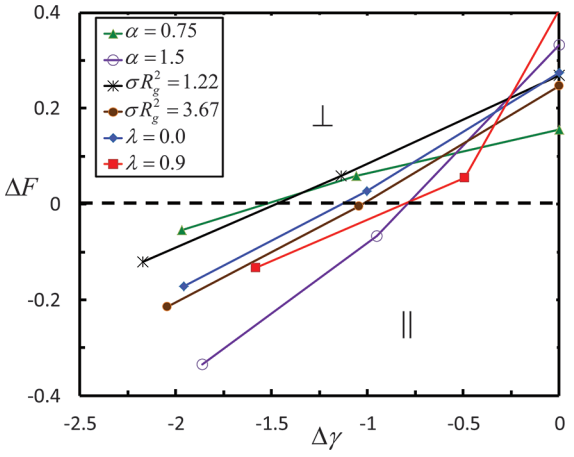

Figure 12. ΔF and $\Delta\gamma$ for different grafting densities σ and blockiness λ. Different σs correspond to $\lambda = 0$, and different λs are for $\sigma R_g^2 = 2.45$. The different points for each parametric condition correspond to brushes with $f = 0.5$,0.6 and 0.7 (representing increasingly A-rich random copolymers). $\perp$ and $\parallel$ denote regions of stability for the respective alignments.

The results of parts a−c of Figure 11 can again be rationalized by invoking the primary mechanism underlying the free energy differences, namely the differences between the interfacial enrichments observed in the parallel and perpendicular alignment of the lamellae. We suggested that such differences were determined by an interplay of the entropic costs of splaying the chain and the enthalpic gain achievable by the enhanced enrichment. We hypothesize that beyond a certain grafting density σ, the entropic cost of splaying would become less sensitive to σ, and consequently, changing σ would have only little impact upon the differences in the interfacial enrichments between parallel and perpendicular alignments.

Finally, in Figure 12, we collate our results (including results for varying α, which was not explicitly discussed) for $\Delta\gamma$ and ΔF to address whether the surface free energies (and their differences) determined on the homopolymer components, can be used as a quantitative indicator of the stability of alignment of morphologies. In agreement with the trends seen in the other results presented in this section, we observe that there is an enhanced regime of stability for perpendicularly aligned lamella ($\Delta F > 0$) extending to significantly non-neutral surfaces ($\Delta\gamma < 0$). More importantly, it is seen that while there is a general trend that smaller $|\Delta\gamma|$s lead to perpendicularly aligned lamella, the correspondence between the two quantities is not unique. Indeed, we observe conditions where a specified $\Delta\gamma$ may result in $\Delta F > 0$ (perpendicular morphologies being preferred) or $\Delta F < 0$ (parallel morphologies being preferred), indicating the differing stabilities of parallel and perpendicular alignment. These considerations confirm that the morphology-driven interfacial interactions endow nontrivial stability characteristics for the different phases which cannot be uniquely correlated to the surface energy values of the homopolymeric components.

V. CONCLUSIONS

In this article, we used SCFT to explore the phase behavior of a diblock copolymer thin film on a substrate grafted with random copolymers. At the outset, we discussed the qualitative features of the morphologies of the parallel and perpendicularly aligned lamellae formed on such grafted surfaces. For parallel morphologies,

we showed the occurrence of "chemical templating" in the grafted polymers, which manifests as an enrichment in the brush interfacial layer of the component of the diblock copolymer in contact. In the case of perpendicular alignment of the diblock copolymer, we demonstrated that there is an additional possibility of physical templating which leads to lateral inhomogeneities in the heights of the brush. Moreover, we also presented results and rationalized the existence of a more pronounced chemical templating effect during perpendicular alignment of lamellae.

We quantified our morphological considerations by comparing the free energies of parallel and perpendicular alignment as a function of the confinement thickness. We demonstrate that, as a function of film thickness, they exhibit trends that are consistent with previously shown results for parallel and perpendicular morphologies on hard surfaces. However, a key difference is a lack of degeneracy in the free energies of the perpendicular and parallel alignments arising due to the ability of the grafted copolymers to modulate their interfacial interaction in response to the morphology of self-assembly. Additionally, we explored the behavior of the neutral window and found that, in general, this window is larger for more blockier chains and for smaller values of σ. We also sought to assess whether knowledge of the surface energy between the brush and a homopolymer suffices to describe the free energy differences between the parallel and perpendicular alignments as well as their stabilities. We found a lack of correlation between our results for $\Delta\gamma$ and ΔF, which indicates that surface energy considerations alone cannot be used to make predictions about phase behavior of the diblock copolymer thin film.

While the above results were for lamellar phases, we expect even richer behavior to manifest when other self-assembly morphologies and/or the behavior of multiblock copolymers are considered. From an experimental perspective, our results suggest caution in using surface energy measurements to draw conclusions regarding the stability and mechanisms of self-assembly on grafted substrates. From a theoretical perspective, our results indicate that self-assembly on grafted polymer substrates possesses several novel features not captured by modeling them as smooth, confining surfaces, and motivate consideration of similar models for a wider class of systems.

APPENDIX A: DETAILS OF THEORETICAL AND NUMERICAL METHODS

We use self-consistent field theory for tethered polymer chains[48] to determine the structure of a grafted layer of statistical copolymers composed of segments denoted A and B which interacts with an AB diblock copolymer. While previous articles have already detailed the theoretical framework appropriate for similar situations,[49,50] for the sake of completeness we present the pertinent equations and details of the accompanying numerical method. The polymers are modeled as Gaussian chains whose conformations are described by continuous functions $\mathbf{R}_i(s)$ and $\mathbf{R}_j(s)$, where i denotes the free chains and takes on values from 1 to n_f (the number of free chains), and j denotes the grafted chains and runs from 1 to n_g (the number of grafted chains). The variable s is a continuous chain index coordinate running from 0 to N_f for the free chains, where N_f denotes the chain length of free chains, and running from 0 to N_g for the grafted chains, where N_g denotes the number of segments in the grafted chains. For simplicity, we assume that the segmental densities of all the segments are identical and denote it as ρ_0. Using this notation, the partition function of the system in the canonical ensemble can be expressed as

$$Z = \int \prod_{i=1}^{n_f} D\mathbf{R}_i(s) \int \prod_{j=1}^{n_g} D\mathbf{R}_j(s) \exp(-\beta U_0[\mathbf{R}_i(s)] - \beta U_0[\mathbf{R}_j(s)] - \beta U_1[\mathbf{R}_i(s), \mathbf{R}_j(s)])\delta(\hat{\rho}_A + \hat{\rho}_B - \rho_0) \quad \text{(A1)}$$

where $\hat{\rho}_A$ and $\hat{\rho}_B$ denote the microscopic densities of A and B chains, respectively. Also, $\hat{\rho}_A = \hat{\rho}_{A,g} + \hat{\rho}_{A,f}$, where $\hat{\rho}_{A,g}$ and $\hat{\rho}_{A,f}$ are the microscopic densities of component A arising from the grafted and free chains, respectively. The density of B segments is calculated similarly as $\hat{\rho}_B = \hat{\rho}_{B,g} + \hat{\rho}_{B,f}$. The delta function in eq A1 enforces the incompressibility of the overall system by requiring that the sum of the A and B species densities, $\hat{\rho}_A$ and $\hat{\rho}_B$, equals the average melt system density ρ_0. In eq A1, U_0 corresponds to the bonded elastic interactions and, in the Gaussian chain model we adopt, is modeled by a form:[51]

$$\beta U_0[\mathbf{R}_i(s)] = \frac{3}{2b^2} \sum_{i=1}^{n_g} \int_0^{N_f} \mathrm{d}s \left| \frac{\partial \mathbf{R}_i(s)}{\partial s} \right|^2 \quad \text{(A2)}$$

where b denotes the statistical segment length. U_1 describes the nonbonded interactions, in particular the energetic repulsion between chemically dissimilar chains. We adopt a simple Flory model where

$$\beta U_1[\mathbf{R}_i(s)] = v_0 \chi \int \mathrm{d}r\, \hat{\rho}_A \hat{\rho}_B \quad \text{(A3)}$$

with the Flory parameter χ quantifying the energetic penalty associated with the contact of chemically dissimilar segments.

The functional eq A1 can be transformed by using functional integral methods into a field theory in which the fundamental degrees of freedom are potential fields $w_+(\mathbf{r})$and $w_-(\mathbf{r})$,[52] such that

$$Z = \int Dw_+ \int Dw_- \exp(-\beta H[w_+(\mathbf{r}), w_-(\mathbf{r})]) \quad \text{(A4)}$$

where H is an "effective" Hamiltonian given by

$$\frac{H[w_+(\mathbf{r}), w_-(\mathbf{r})]}{k_B T C A} = \int \mathrm{d}z \left[\frac{1}{\chi N_g} w_-^2 + i w_+ + \frac{\chi N_g}{4} \right] - \frac{V_h}{\alpha A} \ln Q_f[-iw_+ - w_-, -iw_+ + w_-] - \frac{\overline{\sigma}}{C} \ln Q_g[-iw_+ - w_-, -iw_+ + w_-]$$

In eq A5, length scales have been nondimensionalized by the unperturbed radius of gyration, $R_g = N_g^{1/2} b/6^{1/2}$, of the grafted chains. This results in a nondimensionalization of the grafting density σ (defined as chains per area) to $\overline{\sigma} = \sigma R_g^2$. The potentials w_+ and w_- and the continuous chain index s have been rescaled by N_g. With this nondimensionalization, the constant $C = \rho_0 R_g^d / N_g$ and $\alpha = N_f/N_g$ emerge as dimensionless parameters. Given the total system volume V and the cross sectional area A of the film (all dimensionless), we define the volume of the homopolymer melt V_h by the relationship $V/A = V_h/A + \overline{\sigma}/C$. Q_g is the partition function of a single grafted chain in the fields $w_+(\mathbf{r})$ and $w_-(\mathbf{r})$, and is defined as

$$Q_g(\mathbf{r}_\perp; [\psi]) = \int \mathrm{d}\mathbf{r}\, q_{\mathbf{r}_\perp}(\mathbf{r}, s; [\psi]) \quad \text{(A5)}$$

In the above equation, the field $q_{r\perp}(\mathbf{r},s;[\psi])$, referred to as the chain propagator, provides a statistical description of grafted

chain conformations and satisfies a diffusion-like equation[52]

$$\frac{\partial q_{\mathbf{r}_\perp}}{\partial s} = \nabla^2 q_{\mathbf{r}_\perp} - \psi(\mathbf{r},s;\theta(s))q_{\mathbf{r}_\perp}; \quad q_{\mathbf{r}_\perp}(\mathbf{r},s=0) = \delta(\mathbf{r}-\mathbf{r}_\perp) \tag{A6}$$

The initial condition in eq A6 is the result of the fact that one end of the chain is grafted to the surface, denoted by $\mathbf{r}_\perp$. The potential $\psi(\mathbf{r},s)$ is the potential field acting on the different monomers and is based on the statistical distribution of the monomers. If we use the definition of a random variable $\theta(s)$ that takes on a value of 1 for an A monomer and 0 for a B monomer, then

$$\psi(\mathbf{r},s;\theta(s)) = \begin{cases} -iw_+(\mathbf{r}) - w_-(\mathbf{r}), & \text{if } \theta(s) = 1 \\ -iw_+(\mathbf{r}) + w_-(\mathbf{r}), & \text{if } \theta(s) = 0 \end{cases} \tag{A7}$$

We note that, as discussed further below, experimental conditions dictate that $\theta(s)$ is different for each chain in the system. The equations presented here reflect our implementation of the SCFT for one realization of $\theta(s)$, and we discuss below how this construction is used to model the presence of many chemically distinct chains in the system. Q_f is the partition function of a single free chain in the field $w(\mathbf{r})$ and is defined as

$$Q_f = \int \mathrm{d}\mathbf{r}\, q_f(\mathbf{r}, s=\alpha) \tag{A8}$$

The field $q_f(r,s)$ also satisfies a diffusion equation

$$\frac{\partial q_f(\mathbf{r},s)}{\partial s} = \nabla^2 q_f(\mathbf{r},s) - \xi(\mathbf{r},s)q_f(\mathbf{r},s); q_f(\mathbf{r},s=0) = 1 \tag{A9}$$

where

$$\xi(\mathbf{r},s) = \begin{cases} -iw_+(\mathbf{r}) - w_-(\mathbf{r}), & 0 \le s \le f_{diblock}\alpha \\ -iw_+(\mathbf{r}) + w_-(\mathbf{r}), & f_{diblock}\alpha < s \le \alpha \end{cases} \tag{A10}$$

The potential field in the above equation arises as a consequence of the fact that the free chains are assumed to be AB diblock copolymer chains with volume fraction $f_{diblock}$. The volume fraction profiles of the melt chains, composed of species A and B segments, are defined as $\phi_{A,f} = \rho_{A,f}/\rho_0$ and $\phi_{B,f} = \rho_{B,f}/\rho_0$, respectively. They are obtained as

$$\phi_{A,f}(\mathbf{r}) = \frac{V_h}{VQ_f\alpha}\int_0^{f_{diblock}\alpha} \mathrm{d}s\, q_f(\mathbf{r},s)q_f(\mathbf{r},1-s) \tag{A11}$$

and

$$\phi_{B,f}(\mathbf{r}) = \frac{V_h}{VQ_f\alpha}\int_{f_{diblock}\alpha}^{\alpha} \mathrm{d}s\, q_f(\mathbf{r},s)q_f(\mathbf{r},1-s) \tag{A12}$$

The single chain partition function of the grafted chains, Q_g, can be rewritten using a factorization property as[48]

$$Q_g(\mathbf{r}_\perp) = \int \mathrm{d}\mathbf{r}\, q_{\mathbf{r}_\perp}(\mathbf{r},s)q_g(\mathbf{r},1-s) \tag{A13}$$

where $q_g(\mathbf{r},s)$ is a complementary chain propagator that satisfies eq A6 with an initial condition of $q_g(\mathbf{r},s=0) = 1$. A further complementary propagator can be defined as

$$q_{gc}(\mathbf{r},s) = \int \mathrm{d}\mathbf{r}_\perp \frac{\overline{\sigma} q_{\mathbf{r}_\perp}(\mathbf{r},s)}{Q g(\mathbf{r}_\perp,s)} \tag{A14}$$

which can be shown to satisfy eq A6 with, however, an initial condition

$$q_{gc}(\mathbf{r},s=0) = \frac{\overline{\sigma}\delta(\mathbf{r}-\mathbf{r}_\perp)}{q_g(\mathbf{r}=\mathbf{r}_\perp,s=1)} \tag{A15}$$

The volume fraction profiles of species A and B in the brush, $\phi_{A,g}(\mathbf{r})$ and $\phi_B(\mathbf{r})$ (also normalized by ρ_0), are then found as

$$\phi_{A,g}(\mathbf{r}) = \int_0^1 \mathrm{d}s\, \theta(s)q_{gc}(\mathbf{r},s)q_g(\mathbf{r},1-s) \tag{A16}$$

and

$$\phi_{B,g}(\mathbf{r}) = \int_0^1 \mathrm{d}s\, (1-\theta(s))q_{gc}(\mathbf{r},s)q_g(\mathbf{r},1-s) \tag{A17}$$

Replacing eq A4 with the value of the exponent at its saddle point constitutes the approximation termed as self-consistent field theory (SCFT). The saddle point fields, w^*_+ and w^*_-, found by setting the functional derivative of eq A5 with respect to $w_+(\mathbf{r})$ and $w_-(\mathbf{r})$ to be zero, correspond to the solutions of the equations

$$1 - \phi_A(\mathbf{r}) - \phi_B(\mathbf{r}) = 0 \tag{A18}$$

and

$$\phi_A - \phi_B - (2/\chi N)w^*_- = 0. \tag{A19}$$

The free energy of the system can then be approximated using the value of $H[w_+{}^*(r),w_-{}^*(r)]$ at the saddle point as

$$\frac{F[w(\mathbf{r})]}{k_B TAC} = \frac{-\ln Z}{AC} = \int \mathrm{d}\mathbf{r}\left[\frac{1}{\chi N}w^{*2}_- + iw^*_+ + \frac{\chi N}{4}\right] - \frac{V_h}{\alpha A}\ln Q_f - \frac{\overline{\sigma}}{C}\ln Q_g \tag{A20}$$

Computation of F requires the solution of eqs A6−A13 and A15−A19 with the appropriate boundary conditions. As discussed in previous theoretical studies in the context of thin films,[49] we use a reflecting wall boundary condition at the top of the film, which describes the symmetry condition at half the confinement thickness. This dictates that we impose Neumann boundary conditions, $\mathbf{n}\cdot\nabla q_f = \mathbf{n}\cdot\nabla q_g = \mathbf{n}\cdot\nabla q_{gc} = 0$ at this surface. For numerical reasons discussed in our previous work,[53] instead of using the Dirichlet boundary conditions on the grafted surface, we use a Neumann boundary condition on this surface.

The saddle point fields $w_+(\mathbf{r})$ and $w_-(\mathbf{r})$ are determined using a Picard iterative scheme of the form

$$w^*_+(\mathbf{r})_{new} = w^*_+(\mathbf{r})_{old} + \varepsilon_+[1 - \phi_f(\mathbf{r}) - \phi_g(\mathbf{r})] \tag{A21}$$

and

$$w^*_-(\mathbf{r})_{new} = w^*_-(\mathbf{r})_{old} + \varepsilon_-[\phi_A - \phi_B - (2/\chi N)W_-] \tag{A22}$$

where ε_+ and ε_- are relaxation parameters whose values were chosen to be between 0 and 1. Additionally, the average value of w_+ is enforced to be zero at every iteration.

Mimicking the experimental conditions involving statistical copolymers requires us to generate a "quenched" ensemble of chains whose overall composition of species A is represented by the parameter f but with a distribution of sequences reflecting the statistical nature of their sequences. For this purpose, we use the construction of Fredrickson et al.[54] to generate our copolymers. A parameter P_{jk} is defined as the conditional probability that a

segment of type j at an arbitrary location in the chain is immediately followed by a segment of type k, where j,k = A or B. Because the only options that exist are A or B segments, by construction $P_{AB} = 1 - P_{AA}$ and $P_{BA} = 1 - P_{BB}$. Also, to ensure that the average volume fraction of the segments is f, we have $f = P_{AA}f + P_{BA}(1 - f)$. Given these equalities, it can be shown that the resulting statistical distribution of sequences on the chains can be described by the parameter $\lambda = P_{AA} + P_{BB} - 1$ and that $P_{AA} = f(1 - \lambda) + \lambda$ and $P_{BB} = f(\lambda - 1) + 1$. The parameter λ quantifies the tendency of a new segment to remain chemically equivalent to the previous one. Specifically, $\lambda = 0$ corresponds to the purely random case, $\lambda = -1$ corresponds to an alternating copolymer, and $\lambda = 1$ corresponds to a homopolymer with chemical identity determined by the probability associated with the first segment in the chain. To implement this strategy, we generate an ensemble of chains based on the above procedure and average the results over them to account for the statistical nature of sequences in the polymers.

Since the numerical discretization "Δs" is distinct from the physical size of a segment in the chain, we also specify the number of segments in the chain and generate "segments" composed of the appropriate number of s points. The SCFT calculations are then performed on all n_g of these chains and the results averaged at each iteration. For each parameter set, we did a run on 500 chains composed of 100 segments and averaged the results. Given that $\Delta s = 0.005$ and $0 < s < 1$, this means that each segment is composed of 2 s points.

To quantify the interfacial energy between the bulk film and the brush, we use an approach similar to that expounded in Matsen.[49] Explicitly, the free energy of the system $F(d)$ is calculated as a function of the total film thickness d (which includes both free and grafted chains). Subsequently, the interfacial energy between the bulk diblock copolymer film and the brush is obtained as[49]

$$\gamma_{b/d} = \frac{F(\infty) - F(d_{\min})}{A} \tag{A23}$$

where d_{min} is the thickness for which $F(d)$ is a minimum and A is the area of the substrate. Using eq A23, we obtain values of $\gamma_{b/d}$ at different values of f, denoted $\gamma(f)$. We then assume that, since the substrate interacts neutrally with both chemical components in the system, $\gamma(f) = \gamma_A$ and $\gamma(1 - f) = \gamma_B$. We calculate $\Delta\gamma = \gamma(f) - \gamma(1 - f)$ as a way of quantifying the relative preference for the brush of components A and B in the melt.

AUTHOR INFORMATION

Corresponding Author
*Email: venkat@che.utexas.edu.

ACKNOWLEDGMENT

The authors would like to acknowledge Dr. Manas Shah and Prof. David Wang for helpful discussions. This work was supported by National Science Foundation (1005739), by a grant from Robert A. Welch Foundation (Grant F1599) and the US Army Research Office under Grant W911NF-10-1-0346. The authors acknowledge the Texas Advanced Computing Center (TACC) at The University of Texas at Austin for providing computing resources that have contributed to the research results reported within this paper.

REFERENCES

(1) Ruiz, R.; Kang, H.; Detcheverry, F.; Dobisz, E.; Kercher, C.; Albrecht, T.; de Pablo, J.; Nealey, P. *Science* **2008**, *321*, 936.
(2) Morkved, T.; Lu, M.; Urbas, A.; Ehrichs, E.; Jaeger, H.; Mansky, P.; Russell, T. *Science* **1996**, *273*, 931.
(3) Thurn-Albrecht, T.; Schotter, J.; Kastle, G.; Emley, N.; Shibauchi, T.; Krusin-Elbaum, L.; Guarini, K.; Black, C.; Tuominen, M.; Russell, T. *Science* **2000**, *290*, 2126.
(4) Mansky, P.; Liu, Y.; Huang, E.; Russell, T. P.; Hawker, C. *Science* **1997**, *275*, 1458.
(5) Mansky, P.; Russell, T.; Hawker, C.; Pitsikalis, M.; Mays, J. *Macromolecules* **1997**, *30*, 6810.
(6) Huang, E.; Russell, T.; Harrison, C.; Chaikin, P.; Register, R.; Hawker, C.; Mays, J. *Macromolecules* **1998**, *31*, 7641.
(7) Hamley, I. W. *Prog. Polym. Sci.* **2009**, *34*, 1161.
(8) Bates, C. M.; Strahan, J. R.; Santos, L. J.; Mueller, B. K.; Bamgbade, B. O.; Lee, J. A.; Katzenstein, J. M.; Ellison, C. J.; Willson, C. G. *Langmuir* **2011**, *27*, 2000.
(9) Turner, M. *Phys. Rev. Lett.* **1992**, *69*, 1788.
(10) Pickett, G.; Witten, T.; Nagel, S. *Macromolecules* **1993**, *26*, 3194.
(11) Walton, D.; Kellogg, G.; Mayes, A.; Lambooy, P.; Russell, T. *Macromolecules* **1994**, *27*, 6225.
(12) Shull, K. *Macromolecules* **1992**, *25*, 2122.
(13) Pickett, G.; Balazs, A. *Macromolecules* **1997**, *30*, 3097.
(14) Matsen, M. *J. Chem. Phys.* **1997**, *106*, 7781.
(15) Geisinger, T.; Muller, M.; Binder, K. *J. Chem. Phys.* **1999**, *111*, 5241.
(16) Wang, Q.; Qiliang, Y.; Nealey, P.; de Pablo, J. *J. Chem. Phys.* **2000**, *112*, 450.
(17) Wang, Q.; Nealey, P.; de Pablo, J. *Macromolecules* **2001**, *34*, 3458.
(18) Zhulina, E.; Halperin, A. *Macromolecules* **1992**, *25*, 5730.
(19) Jones, R.; Kane, L.; Spontak, R. *Chem. Eng. Sci.* **1996**, *51*, 1365.
(20) Matsen, M.; Schick, M. *Macromolecules* **1994**, *27*, 187.
(21) Matsen, M.; Thompson, R. *J. Chem. Phys.* **1999**, *111*, 7139.
(22) Drolet, F.; Fredrickson, G. *Macromolecules* **2001**, *34*, 5317.
(23) Shah, M.; Ganesan, V. *Macromolecules* **2010**, *43*, 543.
(24) Wang, Q.; Nath, S.; Graham, M.; Nealey, P.; de Pablo, J. *J. Chem. Phys.* **2000**, *112*, 9996.
(25) Wang, Q.; Yan, Q.; Nealey, P.; de Pablo, J. *Macromolecules* **2000**, *33*, 4512.
(26) Wang, Q. *Macromol. Theory Simul.* **2005**, *14*, 96.
(27) Detcheverry, F.; Liu, G.; Nealey, P.; de Pablo, J. *Macromolecules* **2010**, *43*, 3446.
(28) Detcheverry, F.; Nealey, P.; de Pablo, J. *Macromolecules* **2010**, *43*, 6495.
(29) Tsori, Y.; Andelman, D. *Macromolecules* **2003**, *36*, 8560.
(30) Meng, D.; Wang, Z. *Soft Matter* **2010**, *6*, 5819.
(31) Ferreira, P.; Leibler, L. *J. Chem. Phys.* **1996**, *105*, 9362.
(32) Dong, A.; Marko, J. F.; Witten, T. A. *Macromolecules* **1994**, *27*, 6428.
(33) Brown, G.; Chakrabarti, A.; Marko, J. *Macromolecules* **1995**, *28*, 7817.
(34) Matsen, M.; Griffiths, G. *Eur. Phys. J. E* **2009**, *29*, 219.
(35) Seifpour, A.; Spicer, P.; Nair, N.; Jayaramana, A. *J. Chem. Phys.* **2010**, *132*, 164901.
(36) Griffiths, G. H.; Vorselaars, B.; Matsen, M. W. *Macromolecules* **2011**, *44*, 3649.
(37) Vorselaars, B.; Kim, J. U.; Chantawansri, T. L.; Fredrickson, G. H.; Matsen, M. W. *Soft Matter* **2011**, *7*, 5128.
(38) Zhulina, E.; Balazs, A. C. *Macromolecules* **1996**, *29*, 2667.
(39) Marko, J. F.; Witten, T. A. *Macromolecules* **1992**, *25*, 296.
(40) Brown, G.; Chakrabarti, A.; Marko, J. *Europhys. Lett.* **1994**, *25*, 239.
(41) Lai, P.-Y. *J. Chem. Phys.* **1994**, *100*, 3351.
(42) Muller, M. *Phys. Rev. E* **2002**, *65*, 030802.
(43) Pickett, G. T. *J. Chem. Phys.* **2003**, *118*, 3898.

(44) Gersappe, D.; Fasolka, M.; Israels, R.; Balazs, A. C. *Macromolecules* **1995**, *28*, 4753.
(45) Trombly, D.; Pryamitsyn, V.; Ganesan, V. *J. Chem. Phys.* **2011**, *134*, 154903.
(46) Ren, C.; Chen, K.; Ma, Y. *J. Chem. Phys.* **2005**, *122*, 154904.
(47) Trombly, D.; Pryamitsyn, V.; Ganesan, V. *Phys. Rev. Lett.* **2011**, *107*, 148304.
(48) Fredrickson, G., *The Equilibrium Theory of Inhomogeneous Polymers*; Oxford University Press: Oxford, U.K., 2006.
(49) Matsen, M. W.; Gardiner, J. M. *J. Chem. Phys.* **2001**, *115*, 2794.
(50) Matsen, M. W.; Gardiner, J. M. *J. Chem. Phys.* **2003**, *118*, 3775.
(51) Edwards, S. *Proc. Phys. Soc.* **1965**, *85*, 613.
(52) Fredrickson, G. H.; Ganesan, V.; Drolet, F. *Macromolecules* **2002**, *35*, 16.
(53) Trombly, D.; Ganesan, V. *J. Polym. Sci., Part B: Polym. Phys.* **2009**, *47*, 2566.
(54) Fredrickson, G. H.; Milner, S. T.; Leibler, L. *Macromolecules* **1992**, *25*, 6341.